# Efficient $GW$ calculations for $SnO_2$, ZnO, and rubrene: The effective-energy technique

J. A. Berger,[1,3,*] Lucia Reining,[2,3] and Francesco Sottile[2,3]

[1]*Laboratoire de Chimie et Physique Quantiques (UMR 5626 du CNRS), IRSAMC, Université P. Sabatier, 118 Route de Narbonne, F-31062 Toulouse Cedex, France*

[2]*Laboratoire des Solides Irradiés, École Polytechnique, CNRS, CEA-DSM, F-91128 Palaiseau, France*

[3]*European Theoretical Spectroscopy Facility (ETSF)*

(Received 22 December 2011; published 27 February 2012)

In a recent Rapid Communication [J. A. Berger, L. Reining, and F. Sottile, Phys. Rev. B **82**, 041103(R) (2010)], we presented the effective-energy technique to evaluate, in an accurate and numerically efficient manner, electronic excitations by reformulating spectral sum-over-states expressions such that only occupied states appear. In our approach all the empty states are accounted for by a single effective energy that can be obtained from first principles. In this work we provide further details of the effective-energy technique, in particular, when combined with the $GW$ method, in which a huge summation over empty states appears in the calculation of both the screened Coulomb interaction and the self-energy. We also give further evidence of the numerical accuracy of the effective-energy technique by applying it to the technological important materials $SnO_2$ and ZnO. Finally, we use this technique to predict the band gap of bulk rubrene, an organic molecular crystal with a 140-atom unit cell.

DOI: 10.1103/PhysRevB.85.085126 PACS number(s): 71.10.−w, 71.15.Qe, 71.20.−b

## I. INTRODUCTION

Many-body perturbation theory (MBPT) has become the standard tool for the calculation of quasiparticle energies. The fundamental quantity of MBPT is the single-particle Green's function, the poles of which are the electron removal and addition energies of the system. For the study of many-electron systems, such as solids and macromolecules, the state-of-the-art MBPT approximation is Hedin's $GW$[1] method because it takes into account in an accurate and efficient manner the fact that each electron is screened by its Coulomb hole.

However, the $GW$ approach is a computationally demanding method, which limits its application to relatively simple systems. The main reason for this shortcoming is related to the simple but slowly converging sum-over-states (SOS) approach used in standard $GW$ implementations to calculate both the screened Coulomb interaction and the self-energy. The self-energy is the quantity within MBPT that takes into account all the many-body effects beyond the Hartree potential. The SOS approach requires the summation of an, in principle, infinite number of empty states. In practice, this summation is truncated but a huge number of empty states is required to reach numerical convergence.[2–6]

In the past, several approaches have been proposed to overcome this problem of $GW$, beginning with the Coulomb hole plus screened exchange (COHSEX) approximation.[1] The COHSEX self-energy is a static approximation to the $GW$ self-energy which eliminates empty states in the self-energy only, and at the price of a crude description of the quasiparticle energies. The omitted dynamical part can be approximately accounted for by a linear expansion of the $GW$ self-energy with respect to the frequency.[7,8] Alternatively, one can use a Sternheimer type of approach,[9–11] that is in principle exact, for both the screened interaction and the self-energy. However, in its straightforward application, an approximate Taylor expansion around a set of reference energies is necessary to improve on the standard SOS formulation.[11]

In recent years, thanks to an increased interest in the $GW$ method, many advances have been made to eliminate or reduce the number of empty states in $GW$ calculations.[6,12–16] In particular, many efforts have been made to improve the Sternheimer approach for $GW$ calculations by introducing efficient iterative techniques[12–14] and a self-consistent Sternheimer equation.[15] Other recent proposals to speed up $GW$ calculations involve the design of efficient bases[17–19] or the use of simple approximate physical orbitals.[20]

Recently, we presented the effective-energy technique[21] (EET) to reformulate SOS expressions in terms of occupied states only. Within the EET all the empty states are accounted for by a single effective energy. Moreover, we demonstrated that this effective energy can be obtained from first principles and that already simple approximations to the effective energy lead to excellent results.[21] Therefore, the EET is an efficient method that retains the advantages of the SOS approach, such as simplicity and a good prefactor, but eliminates empty states from the calculation, leading to an immediate speedup for all system sizes. In principle, the EET could be used to speed up the calculation of many spectral quantities. The $GW$ method, in particular, benefits from this approach, as an SOS is encountered twice, once for the calculation of the screening and once for the calculation of the self-energy.

The paper is organized as follows. In Sec. II we give a detailed account of the theory behind the EET. In particular, we focus on its application to the efficient calculation of the polarizability and the $GW$ self-energy. In Sec. III we discuss some details of our implementation of the EET. In Sec. IV we show results of the EET for quasiparticle energies and band gaps of $SnO_2$ and ZnO, two materials with interesting electronic applications, in particular, in the field of transparent conducting oxides. We compare these results to those of standard SOS calculations. We then use the EET to predict the band gap of a large molecular crystal, namely, bulk rubrene. Finally, in Sec. V we draw our conclusions.

 

## II. THEORY

In the following we describe in detail how the EET can be used to reformulate both the $GW$ self-energy and the polarizability in terms of occupied states only. We use atomic units everywhere unless stated otherwise and time-reversal symmetry is assumed to hold throughout.

### A. The GW self-energy

The $GW$ self-energy $\Sigma$ is given by the convolution

$$\Sigma(\mathbf{r},\mathbf{r}',\omega) = i\int_{-\infty}^{\infty}\frac{d\omega'}{2\pi}e^{i\eta\omega'}G(\mathbf{r},\mathbf{r}',\omega+\omega')W(\mathbf{r},\mathbf{r}',\omega'), \quad (1)$$

where the infinitesimal $\eta$ is to be taken in the limit to 0 after the frequency integration. In the above expression $G(\omega)$ is the single-particle Green's function and $W(\omega)$ is the dynamically screened Coulomb potential given by

$$W(\mathbf{r},\mathbf{r}',\omega) = \int d\mathbf{r}''\frac{\epsilon^{-1}(\mathbf{r},\mathbf{r}'',\omega)}{|\mathbf{r}''-\mathbf{r}'|}, \quad (2)$$

where the inverse dielectric function $\epsilon^{-1}(\omega)$ is defined as

$$\epsilon^{-1}(\mathbf{r},\mathbf{r}',\omega) = \delta(\mathbf{r}-\mathbf{r}') + \int d\mathbf{r}''\frac{\chi(\mathbf{r}'',\mathbf{r}',\omega)}{|\mathbf{r}-\mathbf{r}''|}. \quad (3)$$

The reducible time-ordered polarizability $\chi(\omega)$ is given by

$$\chi(\mathbf{r},\mathbf{r}',\omega) = \sum_{g=1}^{\infty}\frac{2\omega_g n_g(\mathbf{r})n_g(\mathbf{r}')}{\omega^2-\omega_g^2}, \quad (4)$$

where $\omega_g = E(N,g) - E(N,0) - i\eta$ are the neutral excitation energies of the $N$-electron system minus an infinitesimal $i\eta$, which ensures the correct time ordering, and $n_g$ are the corresponding oscillator strengths. To keep our formalism general we do not yet make any assumptions on the excitation energies and oscillator strengths and, therefore, on the dielectric function. From Sec. II C onward we employ the usual random-phase approximation (RPA) for the dielectric function, which is generally associated with the $GW$ approximation. In standard $GW$ calculations the Green's function in Eq. (1) is replaced by a zero-order or independent-particle Green's function $G_0(\omega)$ which, in its spectral representation, reads

$$G_0(\mathbf{r},\mathbf{r}',\omega) = \sum_{i=1}^{\infty}\frac{\phi_i(\mathbf{r})\phi_i^*(\mathbf{r}')}{\omega-\varepsilon_i-i\eta\,\mathrm{sgn}(\mu-\varepsilon_i)}, \quad (5)$$

where $\phi_i(\mathbf{r})$ and $\varepsilon_i$ are quasiparticle wave functions and energies, respectively, and $\mu$ is the chemical potential. Although the method that we describe in this work is valid for both finite systems and extended systems described by periodic boundary conditions, we focus here on the latter. Therefore the index $i$ in Eq. (5) should be considered a multi-index composed of the band index, the spin, and the Bloch vector. The substitution of $G_0(\omega)$ for $G(\omega)$ in Eq. (1) permits us to carry out analytically the frequency integration in Eq. (1), giving[22]

$$\Sigma(\mathbf{r},\mathbf{r}',\omega) = \Sigma_x(\mathbf{r},\mathbf{r}'\omega) + \Sigma_c(\mathbf{r},\mathbf{r}'\omega), \quad (6)$$

$$\Sigma_x(\mathbf{r},\mathbf{r}',\omega) = \sum_{i=1}^{\infty}\theta(\mu-\varepsilon_i)\frac{\phi_i(\mathbf{r})\phi_i^*(\mathbf{r}')}{|\mathbf{r}-\mathbf{r}'|}, \quad (7)$$

$$\Sigma_c(\mathbf{r},\mathbf{r}',\omega) = \sum_{i=1}^{\infty}\sum_{g=1}^{\infty}\frac{V^g(\mathbf{r})V^g(\mathbf{r}')\phi_i(\mathbf{r})\phi_i^*(\mathbf{r}')}{\omega+\omega_g\,\mathrm{sgn}(\mu-\varepsilon_i)-\varepsilon_i}, \quad (8)$$

where we divided the self-energy into an exchange ($\Sigma_x$) and a correlation ($\Sigma_c$) part and where $V^g(\mathbf{r}) = \int d\mathbf{r}' n_g(\mathbf{r}')/|\mathbf{r}-\mathbf{r}'|$ are fluctuation potentials. Only the correlation part of the self-energy implies a summation over all the empty states, and therefore we only consider this part of the self-energy in the following.

In standard $GW$ calculations[23,24] the quasiparticle energies are obtained from first-order perturbation theory, where the perturbation is given by the difference between the $GW$ Hamiltonian and the Kohn-Sham (KS) Hamiltonian of density-functional theory (DFT),[25,26] i.e., $\Sigma(\mathbf{r},\mathbf{r}',\omega) - v_{\mathrm{xc}}(\mathbf{r})$, with $v_{\mathrm{xc}}(\mathbf{r})$ the exchange-correlation potential of DFT:

$$\varepsilon_n = \varepsilon_n^{\mathrm{KS}} + Z_n\langle\phi_n^{\mathrm{KS}}|\Sigma(\varepsilon_n^{\mathrm{KS}}) - v_{\mathrm{xc}}|\phi_n^{\mathrm{KS}}\rangle, \quad (9)$$

where the renormalization factor $Z_n$ is given by

$$Z_n = \left[1 - \frac{\partial\langle\phi_n^{\mathrm{KS}}|\Sigma(\omega)|\phi_n^{\mathrm{KS}}\rangle}{\partial\omega}\bigg|_{\omega=\varepsilon_n^{\mathrm{KS}}}\right]^{-1}. \quad (10)$$

Therefore in standard $GW$ calculations one does not require the full knowledge of the spatial dependence of the self-energy but only has to evaluate its diagonal matrix elements. In Eqs. (9) and (10), these matrix elements involve KS wave functions. However, to keep our formulation general, in the following we consider matrix elements of general wave functions which can be the eigenfunctions either of a KS Hamiltonian or of a general static nonlocal Hamiltonian.

### B. The effective-energy technique

The matrix elements of the correlation part $\Sigma_c^n(\omega) \equiv \langle n|\Sigma_c(\omega)|n\rangle$ are given by

$$\Sigma_c^n(\omega) = \sum_{i=1}^{\infty}\sum_{g=1}^{\infty}\frac{|\langle n|V^g|i\rangle|^2}{\omega+\omega_g\,\mathrm{sgn}(\mu-\varepsilon_i)-\varepsilon_i}. \quad (11)$$

The summation over $i$ in Eq. (11) can be split into a summation over occupied states $v$ with $\varepsilon_v < \mu$ and a summation over empty states $c$ with $\varepsilon_c > \mu$. In the following we focus on the latter summation since it is the bottleneck in the calculation of $\Sigma_c^n$ as it sums over the, in principle infinite, empty states of the system. Introducing the Fourier transforms of the fluctuation potentials,

$$V^g(\mathbf{r}) = \sum_{\mathbf{q},\mathbf{G}}V_{\mathbf{G}}^g(\mathbf{q})e^{i(\mathbf{q}+\mathbf{G})\cdot\mathbf{r}}, \quad (12)$$

$$V_{\mathbf{G}}^g(\mathbf{q}) = \frac{1}{\Omega}\int d\mathbf{r}V^g(\mathbf{r})e^{-i(\mathbf{q}+\mathbf{G})\cdot\mathbf{r}}, \quad (13)$$

with $\Omega$ the volume of the system, we can rewrite this part as

$$\Sigma_c^{n,\mathrm{emp}}(\omega) = \sum_{g=1}^{\infty}\sum_{\mathbf{q},\mathbf{G},\mathbf{G}'}V_{\mathbf{G}}^g(\mathbf{q})V_{\mathbf{G}'}^{g*}(\mathbf{q})S_g^n(\mathbf{q},\mathbf{G},\mathbf{G}',\omega), \quad (14)$$

where we defined

$$S_g^n(\mathbf{q},\mathbf{G},\mathbf{G}',\omega) = \sum_c\frac{\tilde{\rho}_{cn}^*(\mathbf{q}+\mathbf{G})\tilde{\rho}_{cn}(\mathbf{q}+\mathbf{G}')}{\omega-\omega_g-\varepsilon_c}, \quad (15)$$

in which $\tilde{\rho}_{cn}(\mathbf{q}+\mathbf{G}) = \langle c|e^{-i(\mathbf{q}+\mathbf{G})\cdot\mathbf{r}}|n\rangle$. It is the above summation over empty states that we eliminate. We now introduce a function $\delta_{ng}(\mathbf{q},\mathbf{G},\mathbf{G}',\omega)$, which is defined by the following equation:

$$S_g^n(\mathbf{q},\mathbf{G},\mathbf{G}',\omega) = \frac{\sum_c \tilde{\rho}^*_{cn}(\mathbf{q}+\mathbf{G})\tilde{\rho}_{cn}(\mathbf{q}+\mathbf{G}')}{\omega-\omega_g-\varepsilon_n-\delta_{ng}(\mathbf{q},\mathbf{G},\mathbf{G}',\omega)}. \quad (16)$$

Such a function can always be found since $\delta_{ng}(\mathbf{q},\mathbf{G},\mathbf{G}',\omega)$ has the same degrees of freedom as the left-hand side of Eq. (16). With the introduction of this function we can use the closure relation, $\sum_c |c\rangle\langle c| = 1 - \sum_v |v\rangle\langle v|$, and we obtain an expression for $S_g^n$ which contains a summation over occupied states only. The relation in Eq. (16) is exact; the effective energy $\varepsilon_n + \delta_{ng}(\mathbf{q},\mathbf{G},\mathbf{G}',\omega)$ takes into account the contributions of all the empty states to $S_g^n(\mathbf{q},\mathbf{G},\mathbf{G}',\omega)$. For this reason we have named this approach the effective-energy technique (cf. the common-energy denominator approximation).[27] It now remains to find accurate approximations to $\delta_{ng}(\mathbf{q},\mathbf{G},\mathbf{G}',\omega)$ that do not contain any summations over empty states. In the following we show that such approximations can be obtained from first principles. Subtracting Eq. (16) from Eq. (15), and putting the right-hand side over a common denominator, we obtain

$$0 = \sum_c \left[\frac{\tilde{\rho}^*_{cn}(\mathbf{q}+\mathbf{G})\tilde{\rho}_{cn}(\mathbf{q}+\mathbf{G}')}{[\omega-\omega_g-\varepsilon_c]} \frac{(\varepsilon_c-\varepsilon_n-\delta_{ng}(\mathbf{q},\mathbf{G},\mathbf{G}',\omega))}{[\omega-\omega_g-\varepsilon_n-\delta_{ng}(\mathbf{q},\mathbf{G},\mathbf{G}',\omega)]}\right]. \quad (17)$$

Multiplying the above equation by $[\omega-\omega_g-\varepsilon_n-\delta_{ng}(\omega)]$ and rearranging, we arrive at

$$\delta_{ng}(\mathbf{q},\mathbf{G},\mathbf{G}',\omega)S_g^n(\mathbf{q},\mathbf{G},\mathbf{G}',\omega) = \sum_c \frac{\tilde{\rho}^*_{cn}(\mathbf{q}+\mathbf{G})\tilde{\rho}_{cn}(\mathbf{q}+\mathbf{G}')(\varepsilon_c-\varepsilon_n)}{\omega-\omega_g-\varepsilon_c} \quad (18)$$

$$= \frac{1}{2}\sum_c \frac{\tilde{\rho}^*_{cn}(\mathbf{q}+\mathbf{G})\langle c|[\hat{H}(\mathbf{r}'),e^{-i(\mathbf{q}+\mathbf{G}')\cdot\mathbf{r}'}]|n\rangle + \text{H.c.}}{\omega-\omega_g-\varepsilon_c}, \quad (19)$$

where H.c. denotes the Hermitian conjugate. In the last step, we made use of the fact that the $\varepsilon_i$ are eigenvalues of the Hamiltonian $\hat{H}(\mathbf{r})$ with eigenstates $|i\rangle$.[8] Here we consider a Hamiltonian that contains only a local potential, i.e., $\hat{H}(\mathbf{r}) = -\nabla^2_{\mathbf{r}}/2 + v(\mathbf{r})$. The derivation that follows can be easily generalized to include Hamiltonians with additional nonlocal potentials (see Appendix A for further details). We note that the symmetrization we carried out in the numerator of Eq. (19) ensures that the approximations for $\delta_{ng}(\omega)$ that we derive in the following have the correct symmetry.

Working out the commutator in Eq. (19) and dividing both sides by $S_g^n$, we obtain

$$\delta_{ng}(\mathbf{q},\mathbf{G},\mathbf{G}',\omega) = Q(\mathbf{q},\mathbf{G},\mathbf{G}') + \frac{\tilde{S}_g^n(\mathbf{q},\mathbf{G},\mathbf{G}',\omega)}{S_g^n(\mathbf{q},\mathbf{G},\mathbf{G}',\omega)}, \quad (20)$$

where we have defined

$$Q(\mathbf{q},\mathbf{G},\mathbf{G}') = \frac{1}{2}\left[\frac{|\mathbf{q}+\mathbf{G}|^2}{2} + \frac{|\mathbf{q}+\mathbf{G}'|^2}{2}\right], \quad (21)$$

$$\tilde{S}_g^n(\mathbf{q},\mathbf{G},\mathbf{G}',\omega) = \frac{1}{2}\sum_c \frac{\tilde{\rho}^*_{cn}(\mathbf{q}+\mathbf{G})\tilde{j}_{cn}(\mathbf{q}+\mathbf{G}') + \text{H.c.}}{[\omega-\omega_g-\varepsilon_c]}, \quad (22)$$

in which

$$\tilde{j}_{cn}(\mathbf{q}+\mathbf{G}) = \langle c|e^{-i(\mathbf{q}+\mathbf{G})\cdot\mathbf{r}}[i\nabla_{\mathbf{r}}]|n\rangle\cdot(\mathbf{q}+\mathbf{G}). \quad (23)$$

In the case where the Hamiltonian in Eq. (19) contains an additional nonlocal potential $v_{nl}(\mathbf{r},\mathbf{r}')$, the expression for $\tilde{j}_{cn}$ in Eq. (23) has an additional term. This generalized expression for $\tilde{j}_{cn}$ is shown in Eq. (A1). In Eq. (20) $\delta_{ng}$ is expressed in terms of itself through $S_g^n$. Since $\tilde{S}_g^n$ depends on a summation over the empty states, solving for $\delta_{ng}$ will not lead to the desired result. However, in view of the similarity of Eqs. (22) and (15), we can also rewrite Eq. (22) in terms of occupied states only in an equivalent manner to Eq. (16) by defining a modified effective energy $\epsilon_n + \tilde{\delta}_{ng}$ such that

$$\tilde{S}_g^n(\mathbf{q},\mathbf{G},\mathbf{G}',\omega) = \frac{1}{2}\frac{\sum_c \tilde{\rho}^*_{cn}(\mathbf{q}+\mathbf{G})\tilde{j}_{cn}(\mathbf{q}+\mathbf{G}') + \text{H.c.}}{\omega-\omega_g-\varepsilon_n-\tilde{\delta}_{ng}(\mathbf{q},\mathbf{G},\mathbf{G}',\omega)}. \quad (24)$$

Combining the above equation with Eqs. (16) and (20) leads to the following (exact) expression for $\delta_{ng}(\omega)$:

$$\delta_{ng}(\mathbf{q},\mathbf{G},\mathbf{G}',\omega) = Q(\mathbf{q},\mathbf{G},\mathbf{G}') + \frac{f_n^{\rho j}(\mathbf{q},\mathbf{G},\mathbf{G}')}{f_n^{\rho\rho}(\mathbf{q},\mathbf{G},\mathbf{G}')}\frac{\omega_{ng}-\delta_{ng}(\mathbf{q},\mathbf{G},\mathbf{G}',\omega)}{\omega_{ng}-\tilde{\delta}_{ng}(\mathbf{q},\mathbf{G},\mathbf{G}',\omega)}, \quad (25)$$

in which $\omega_{ng} = \omega - \omega_g - \varepsilon_n$ and where

$$f_n^{\rho\rho}(\mathbf{q},\mathbf{G},\mathbf{G}') = -\sum_v \tilde{\rho}^*_{vn}(\mathbf{q}+\mathbf{G})\tilde{\rho}_{vn}(\mathbf{q}+\mathbf{G}') + \tilde{\rho}_{nn}(\mathbf{G}'-\mathbf{G}), \quad (26)$$

$$f_n^{\rho j}(\mathbf{q},\mathbf{G},\mathbf{G}') = \frac{1}{2}\left[-\sum_v \tilde{\rho}^*_{vn}(\mathbf{q}+\mathbf{G})\tilde{j}_{vn}(\mathbf{q}+\mathbf{G}') + \langle n|e^{i(\mathbf{G}-\mathbf{G}')\cdot\mathbf{r}}(i\nabla_{\mathbf{r}})|n\rangle\cdot(\mathbf{q}+\mathbf{G}')\right] + \text{H.c.} \quad (27)$$

$$f_n^{jj}(\mathbf{q},\mathbf{G},\mathbf{G}') = -\sum_v \tilde{j}^*_{vn}(\mathbf{q}+\mathbf{G})\tilde{j}_{vn}(\mathbf{q}+\mathbf{G}') + (\mathbf{q}+\mathbf{G})\cdot\langle\nabla_{\mathbf{r}}n|e^{i(\mathbf{G}-\mathbf{G}')\cdot\mathbf{r}}|\nabla_{\mathbf{r}}n\rangle\cdot(\mathbf{q}+\mathbf{G}'). \quad (28)$$

The expression for $f_n^{jj}$ in Eq. (28) has been added for future reference. In principle, the above procedure could be continued *ad infinitum* by expressing $\tilde{\delta}_{ng}(\omega)$ in Eq. (25) in terms of another effective energy $\epsilon_n + \tilde{\tilde{\delta}}_{ng}(\omega)$, etc. However, one wishes to truncate the expression for $\delta_{ng}$ since, in practice, one would like to use simple expressions. In Ref. 21 we showed that simple expressions already lead to excellent results. To truncate this expression we make use of the fact that, for a homogeneous electron gas, $\delta_{ng} = \tilde{\delta}_{ng}$ (see Appendix B for further details). This motivates our first-order approximation for $\delta_{ng}(\omega)$:

$$\delta_n^{(1)}(\mathbf{q},\mathbf{G},\mathbf{G}') = Q(\mathbf{q},\mathbf{G},\mathbf{G}') + \frac{f_n^{\rho j}(\mathbf{q},\mathbf{G},\mathbf{G}')}{f_n^{\rho\rho}(\mathbf{q},\mathbf{G},\mathbf{G}')}, \quad (29)$$

which is independent of both $g$ and $\omega$. Higher order approximations for $\delta_{ng}(\omega)$ are obtained by continuing the iterative procedure described above and truncating the remaining expression in such a way that the approximate expression

remains exact for a homogeneous electron gas. For example, a second iteration [which introduces $\tilde{\tilde{\delta}}_{ng}(\omega)$] leads to

$$\delta_{ng}(\mathbf{q},\mathbf{G},\mathbf{G}',\omega) = Q(\mathbf{q},\mathbf{G},\mathbf{G}') + \frac{f_n^{\rho j}(\mathbf{q},\mathbf{G},\mathbf{G}')}{f_n^{\rho\rho}(\mathbf{q},\mathbf{G},\mathbf{G}')} \times \left[ \frac{\omega_{ng} - Q(\mathbf{q},\mathbf{G},\mathbf{G}') - \frac{f_n^{\rho j}(\mathbf{q},\mathbf{G},\mathbf{G}')}{f_n^{\rho\rho}(\mathbf{q},\mathbf{G},\mathbf{G}')} \frac{\omega_{ng}-\delta_{ng}(\mathbf{q},\mathbf{G},\mathbf{G}',\omega)}{\omega_{ng}-\tilde{\delta}_{ng}(\mathbf{q},\mathbf{G},\mathbf{G}',\omega)}}{\omega_{ng} - Q(\mathbf{q},\mathbf{G},\mathbf{G}') - \frac{f_n^{jj}(\mathbf{q},\mathbf{G},\mathbf{G}')}{f_n^{\rho j}(\mathbf{q},\mathbf{G},\mathbf{G}')} \frac{\omega_{ng}-\tilde{\delta}_{ng}(\mathbf{q},\mathbf{G},\mathbf{G}',\omega)}{\omega_{ng}-\tilde{\tilde{\delta}}_{ng}(\mathbf{q},\mathbf{G},\mathbf{G}',\omega)}} \right], \tag{30}$$

where $f_n^{jj}$ is given in Eq. (28). Our second-order approximation for $\delta_{ng}(\omega)$ is then motivated by the fact that, for a homogeneous electron gas, $\tilde{\tilde{\delta}}_{ng}(\omega) = \tilde{\delta}_{ng}(\omega) = \delta_{ng}(\omega)$. We now summarize the first three approximations for $\delta_{ng}$ that we obtain:

$$\delta^{(0)}(\mathbf{q},\mathbf{G},\mathbf{G}') = Q(\mathbf{q},\mathbf{G},\mathbf{G}'), \tag{31}$$

$$\delta_n^{(1)}(\mathbf{q},\mathbf{G},\mathbf{G}') = Q(\mathbf{q},\mathbf{G},\mathbf{G}') + \frac{f_n^{\rho j}(\mathbf{q},\mathbf{G},\mathbf{G}')}{f_n^{\rho\rho}(\mathbf{q},\mathbf{G},\mathbf{G}')}, \tag{32}$$

$$\delta_{ng}^{(2)}(\mathbf{q},\mathbf{G},\mathbf{G}',\omega) = Q(\mathbf{q},\mathbf{G},\mathbf{G}') + \frac{f_n^{\rho j}(\mathbf{q},\mathbf{G},\mathbf{G}')}{f_n^{\rho\rho}(\mathbf{q},\mathbf{G},\mathbf{G}')} \times \left[ \frac{\omega_{ng} - Q(\mathbf{q},\mathbf{G},\mathbf{G}') - \frac{f_n^{\rho j}(\mathbf{q},\mathbf{G},\mathbf{G}')}{f_n^{\rho\rho}(\mathbf{q},\mathbf{G},\mathbf{G}')}}{\omega_{ng} - Q(\mathbf{q},\mathbf{G},\mathbf{G}') - \frac{f_n^{jj}(\mathbf{q},\mathbf{G},\mathbf{G}')}{f_n^{\rho j}(\mathbf{q},\mathbf{G},\mathbf{G}')}} \right]. \tag{33}$$

Here we added a simple zero-order approximation which neglects the second term on the right-hand side of Eq. (20). With the second-order expression $\delta_{ng}^{(2)}(\omega)$, we have obtained an approximation which is frequency dependent. The expression for $\delta_{ng}^{(2)}(\omega)$ is therefore nontrivial despite its simple form. Higher order expressions for $\delta_{ng}$ will contain terms with higher order derivatives of the valence wave functions as well as derivatives of the potential. Also, these expressions are, by construction, exact for the homogeneous electron gas. Our results have shown that for inhomogeneous systems these terms can be safely neglected.[21]

### C. The polarizability

In practice, the neutral excitation energies $\omega_g$ and fluctuation potentials $V_{\mathbf{G}}^g(\mathbf{q})$ that enter $\Sigma_c^n(\omega)$ are not known, and as the first step, $\epsilon(\omega)$ has to be calculated. The dielectric function can be expressed in terms of the time-ordered irreducible polarizability $\tilde{\chi}(\omega)$ according to

$$\epsilon(\mathbf{r},\mathbf{r}',\omega) = \delta(\mathbf{r}-\mathbf{r}') - \int d\mathbf{r}'' \frac{\tilde{\chi}(\mathbf{r}'',\mathbf{r}',\omega)}{|\mathbf{r}-\mathbf{r}''|}. \tag{34}$$

Within an approximation that is consistent with the $GW$ approximation for the self-energy, $\tilde{\chi}(\omega)$ is given by a convolution of two Green's functions:

$$\tilde{\chi}(\mathbf{r},\mathbf{r}',\omega) = -i \int d\omega' G(\mathbf{r},\mathbf{r}',\omega+\omega') G(\mathbf{r}',\mathbf{r},\omega'). \tag{35}$$

In standard calculations the Green's functions are replaced by zero-order Green's functions [see Eq. (5)], which leads to $\chi^0(\omega)$, the irreducible polarizability in the RPA. The frequency integral can then be evaluated analytically, which, in reciprocal space, leads to the expression

$$\chi^0_{\mathbf{G}\mathbf{G}'}(\mathbf{q},\omega) = \sum_{s=\pm1} \sum_v n_v X_v(\mathbf{q},\mathbf{G},\mathbf{G}',s\omega) + \sum_{v,v'}^{\text{occ}} (n_v - n_{v'}) \times \frac{\tilde{\rho}^*_{vv'}(\mathbf{q}+\mathbf{G})\tilde{\rho}_{v'v}(\mathbf{q}+\mathbf{G}')}{\omega - (\varepsilon_{v'} - \varepsilon_v) + i\eta \mathrm{sgn}(\epsilon_{v'} - \varepsilon_v)}, \tag{36}$$

in which $n_v$ are occupation numbers and where we have defined

$$X_v(\mathbf{q},\mathbf{G},\mathbf{G}',\omega) = \sum_c \frac{\tilde{\rho}^*_{cv}(\mathbf{q}+\mathbf{G})\tilde{\rho}_{cv}(\mathbf{q}+\mathbf{G}')}{\omega - (\varepsilon_c - \varepsilon_v) + i\eta}. \tag{37}$$

We note that the second term on the right-hand side of Eq. (36) only leads to nonzero contributions in the case of systems with partially occupied bands. Since $X_v(\omega)$ has a structure similar to that of $S_g^n(\omega)$ in Eq. (15), we can also apply the EET to $X_v(\omega)$ and thus obtain an expression for $\chi^0(\omega)$ that does not contain any summations over empty states. Introducing the effective energy $\epsilon_v + \delta'_v(\omega)$, we can rewrite $X_v(\omega)$ as

$$X_v(\mathbf{q},\mathbf{G},\mathbf{G}',\omega) = \frac{f_v^{\rho\rho}(\mathbf{q},\mathbf{G},\mathbf{G}')}{\omega - \delta'_v(\mathbf{q},\mathbf{G},\mathbf{G}',\omega) + i\eta}. \tag{38}$$

To obtain approximations for $\delta'_v(\omega)$ we can follow a strategy similar to that for $\delta_{ng}(\omega)$. The first three approximations that we obtain are

$$\delta'^{(0)}(\mathbf{q},\mathbf{G},\mathbf{G}') = Q(\mathbf{q},\mathbf{G},\mathbf{G}'), \tag{39}$$

$$\delta'^{(1)}_v(\mathbf{q},\mathbf{G},\mathbf{G}') = Q(\mathbf{q},\mathbf{G},\mathbf{G}') + \frac{f_v^{\rho j}(\mathbf{q},\mathbf{G},\mathbf{G}')}{f_v^{\rho\rho}(\mathbf{q},\mathbf{G},\mathbf{G}')}, \tag{40}$$

$$\delta'^{(2)}_v(\mathbf{q},\mathbf{G},\mathbf{G}',\omega) = Q(\mathbf{q},\mathbf{G},\mathbf{G}') + \frac{f_v^{\rho j}(\mathbf{q},\mathbf{G},\mathbf{G}')}{f_v^{\rho\rho}(\mathbf{q},\mathbf{G},\mathbf{G}')} \times \left[ \frac{\omega - Q(\mathbf{q},\mathbf{G},\mathbf{G}') - \frac{f_v^{\rho j}(\mathbf{q},\mathbf{G},\mathbf{G}')}{f_v^{\rho\rho}(\mathbf{q},\mathbf{G},\mathbf{G}')}}{\omega - Q(\mathbf{q},\mathbf{G},\mathbf{G}') - \frac{f_v^{jj}(\mathbf{q},\mathbf{G},\mathbf{G}')}{f_v^{\rho j}(\mathbf{q},\mathbf{G},\mathbf{G}')}} \right]. \tag{41}$$

We note that the zero- and first-order approximations for $\delta'(\omega)$ are identical in form to those for $\delta(\omega)$.

Finally, we note that the expression for $\chi_0(\omega)$ could be further simplified if, instead of approximating $X_v(\omega)$, we approximate $\sum_v n_v X_v(\omega)$. Further details of this simplified EET are given in Appendix C.

### D. Exact constraints

It is known that the RPA polarizability satisfies several sum rules and exact constraints such as the high-frequency limit and the $f$-sum rule. These constraints allow us to obtain more insights in the approximations given by Eqs. (39)–(41). In Sec. II D 1 we show that any approximation $\delta'^{(k)}_v$ with $k > 0$ satisfies the high-frequency limit. However, the same is not true for the $f$-sum rule. While we can show that the first-order approximation $\delta'^{(1)}_v$ satisfies the $f$-sum rule for its diagonal elements (see Sec. II D 2), we cannot do the same for higher order approximations, such as $\delta'^{(2)}_v$. This opens a possible route to construct improved approximations for $\delta'_v(\omega)$. One could

either constrain higher-order approximations to satisfy the $f$-sum rule or find an alternative or additional motivation to the electron-gas argument to truncate $\delta'_v(\omega)$ such that the $f$-sum rule is satisfied. Other exact constraints could be used in a similar way to improve approximations to $\delta'_v(\omega)$ and $\delta_{ng}(\omega)$.[6]

#### 1. The high-frequency limit

The high-frequency limit of $\chi^0(\omega)$ is given by[28]

$$\lim_{\omega\to\infty}\omega^2\chi^0_{\mathbf{GG}'}(\mathbf{q},\omega)=(\mathbf{q}+\mathbf{G})\cdot(\mathbf{q}+\mathbf{G}')\rho(\mathbf{G}'-\mathbf{G}). \quad (42)$$

We now show that this exact constraint remains satisfied when we express $\chi^0(\omega)$ in terms of an effective energy for all approximations $\delta'^{(k)}_v(\mathbf{q},\mathbf{G},\mathbf{G}',\omega)$ with $k>0$.

Performing a Taylor expansion of $\chi^0_{\mathbf{GG}'}(\omega)$ around $\omega=\infty$ yields, for any $k>0$,

$$\chi^0_{\mathbf{GG}'}(\mathbf{q},\omega)=\frac{1}{\omega^2}\left[2\sum_v n_v\left[f_v^{\rho\rho}Q(\mathbf{q},\mathbf{G},\mathbf{G}')+f_v^{\rho j}\right]+\sum_{v,v'}(n_v-n_{v'})\tilde\rho^*_{v'v}(\mathbf{G})\tilde\rho_{v'v}(\mathbf{G}')(\varepsilon_{v'}-\varepsilon_v)\right]+O\left(\frac{1}{\omega^4}\right). \quad (43)$$

For notational convenience, we have suppressed the dependence of $f_v^{\rho\rho}$ and $f_v^{\rho j}$ on $\mathbf{q}$, $\mathbf{G}$, and $\mathbf{G}'$ as well as the dependence of $\tilde\rho_{v'v}$ on $\mathbf{q}$. Using the relation

$$f_v^{\rho\rho}Q(\mathbf{q},\mathbf{G},\mathbf{G}')+f_v^{\rho j}=\sum_c\tilde\rho^*_{cv}(\mathbf{G})\tilde\rho_{cv}(\mathbf{G}')(\varepsilon_c-\varepsilon_v), \quad (44)$$

which can be verified by substitution of Eqs. (26) and (27), we obtain

$$\chi^0_{\mathbf{GG}'}(\mathbf{q},\omega)=\frac{1}{\omega^2}\sum_{n,n'}(n_n-n_{n'})\tilde\rho^*_{n'n}(\mathbf{G})\tilde\rho_{n'n}(\mathbf{G}')(\varepsilon_{n'}-\varepsilon_n)+O\left(\frac{1}{\omega^4}\right) \quad (45)$$

$$=\frac{1}{\omega^2}\sum_n n_n\langle n|[e^{i(\mathbf{q}+\mathbf{G})\cdot\mathbf{r}},[\hat H(\mathbf{r}),e^{-i(\mathbf{q}+\mathbf{G}')\cdot\mathbf{r}}]]|n\rangle+O\left(\frac{1}{\omega^4}\right) \quad (46)$$

$$=\frac{1}{\omega^2}(\mathbf{q}+\mathbf{G})\cdot(\mathbf{q}+\mathbf{G}')\rho(\mathbf{G}'-\mathbf{G})+O\left(\frac{1}{\omega^4}\right). \quad (47)$$

We therefore obtain

$$\lim_{\omega\to\infty}\omega^2\chi^0_{\mathbf{GG}'}(\mathbf{q},\omega)=(\mathbf{q}+\mathbf{G})\cdot(\mathbf{q}+\mathbf{G}')\rho(\mathbf{G}'-\mathbf{G}), \quad (48)$$

which proves that the high-frequency limit is satisfied for all $\delta'^{(k)}_v(\mathbf{q},\mathbf{G},\mathbf{G}',\omega)$ with $k>0$.

#### 2. The $f$-sum rule

The generalized $f$-sum rule is given by[28]

$$\int_0^\infty d\omega\omega\mathrm{Im}\chi^0_{\mathbf{GG}'}(\mathbf{q},\omega)=-\frac{\pi}{2}(\mathbf{q}+\mathbf{G})\cdot(\mathbf{q}+\mathbf{G}')\rho(\mathbf{G}'-\mathbf{G}). \quad (49)$$

We now show that this exact constraint also holds for $\chi^0(\omega)$ when it is expressed in terms of an effective energy using $\delta'^{(1)}_v$ if we assume that $\delta'^{(1)}_v(\mathbf{q},\mathbf{G},\mathbf{G}')$ is both real and non-negative. This assumption holds true for the diagonal elements $\delta'^{(1)}_v(\mathbf{q},\mathbf{G},\mathbf{G})$, as can be verified from Eq. (40). We can now use the relation

$$\lim_{\eta\to0^+}\frac{1}{x\pm i\eta}=\mathcal{P}\frac{1}{x}\mp i\pi\delta(x), \quad (50)$$

where $\mathcal{P}$ denotes the principal value, to write

$$\int_0^\infty d\omega\omega\mathrm{Im}\chi^0_{\mathbf{GG}'}(\mathbf{q},\omega)=-\pi\sum_v n_v f_v^{\rho\rho}\int_0^\infty d\omega\omega\left[\delta\left(\omega-\delta'^{(1)}_v\right)+\delta\left(\omega+\delta'^{(1)}_v\right)\right]-\pi\sum_{v.v'}(n_v-n_{v'})\tilde\rho^*_{v'v}(\mathbf{G})\tilde\rho_{v'v}(\mathbf{G}')\times\int_0^\infty d\omega\omega\delta(\omega-(\varepsilon_{v'}-\varepsilon_v)). \quad (51)$$

For notational convenience, we have suppressed the dependence of $\delta'^{(1)}_v$ and $f_v^{\rho\rho}$ on $\mathbf{q}$, $\mathbf{G}$, and $\mathbf{G}'$ as well as the dependence of $\tilde\rho_{v'v}$ on $\mathbf{q}$. Since, thanks to time-reversal symmetry,

$$\sum_{v.v'}(n_v-n_{v'})\tilde\rho^*_{v'v}(\mathbf{G})\tilde\rho_{v'v}(\mathbf{G}')\int_0^\infty d\omega\omega\delta(\omega-(\varepsilon_{v'}-\varepsilon_v))=\sum_{v.v'}(n_v-n_{v'})\tilde\rho^*_{v'v}(\mathbf{G})\tilde\rho_{v'v}(\mathbf{G}')\int_{-\infty}^0 d\omega\omega\delta(\omega-(\varepsilon_{v'}-\varepsilon_v)), \quad (52)$$

we can write

$$\int_0^\infty d\omega\omega\mathrm{Im}\chi^0_{\mathbf{GG}'}(\mathbf{q},\omega)=-\pi\sum_v n_v f_v^{\rho\rho}\delta'^{(1)}_v-\frac{\pi}{2}\sum_{v.v'}(n_v-n_{v'})\tilde\rho^*_{v'v}(\mathbf{G})\times\tilde\rho_{v'v}(\mathbf{G}')(\varepsilon_{v'}-\varepsilon_v) \quad (53)$$

$$=-\frac{\pi}{2}\sum_{n.n'}(n_n-n_{n'})\tilde\rho^*_{n'n}(\mathbf{G})\tilde\rho_{n'n}(\mathbf{G}')(\varepsilon_{n'}-\varepsilon_n) \quad (54)$$

$$=-\frac{\pi}{2}(\mathbf{q}+\mathbf{G})\cdot(\mathbf{q}+\mathbf{G}')\rho(\mathbf{G}'-\mathbf{G}), \quad (55)$$

where we used Eq. (44). Therefore, the $f$-sum rule is satisfied for $\delta'^{(1)}_v(\mathbf{q},\mathbf{G},\mathbf{G}')$. Using the same procedure we cannot show that the $f$-sum rule is satisfied for $\delta'^{(0)}(\mathbf{q},\mathbf{G},\mathbf{G}')$ and $\delta'^{(2)}_v(\mathbf{q},\mathbf{G},\mathbf{G}',\omega)$

### E. Converging $GW$ calculations

In Ref. 21 we used the EET to obtain approximations to the $GW$ self-energy and the independent-particle polarizability which do not contain summations over empty states. We showed there that simple approximations, such as $\delta^{(2)}(\omega)+\delta'^{(2)}(\omega)$, are accurate and numerically efficient. However, one might wish to converge to the numerically exact $GW$ result. Such numerically exact results can be obtained efficiently and in a systematic way by combining the EET and the SOS approach. Let us illustrate how we achieve this goal for the

self-energy. We first split the expression in Eq. (15) into two parts according to

$$S_g^n(\mathbf{q},\mathbf{G},\mathbf{G}',\omega) = \sum_{c=N_v+1}^{M} \frac{\tilde{\rho}_{cn}^*(\mathbf{q}+\mathbf{G})\tilde{\rho}_{cn}(\mathbf{q}+\mathbf{G}')}{\omega-\omega_g-\varepsilon_c} + \sum_{c=M+1}^{\infty} \frac{\tilde{\rho}_{cn}^*(\mathbf{q}+\mathbf{G})\tilde{\rho}_{cn}(\mathbf{q}+\mathbf{G}')}{\omega_{ng}-\delta_{ng}(\mathbf{q},\mathbf{G},\mathbf{G}',\omega)}, \quad (56)$$

where $N_v$ is the number of occupied states. Here we used the EET only in the second term on the right-hand side, which contains a summation over all the empty states starting from $M+1$. If we choose $M = N_v$, we retrieve Eq. (16). However, if we choose $M > N_v$, the part that needs to be approximated with the EET becomes smaller as $M$ increases. In this way we have obtained an efficient way to converge $S_g^n(\omega)$ with respect to the number of empty states. In a similar way, one can efficiently converge $\chi_0(\omega)$. We note that this procedure is similar to the one proposed by Bruneval and Gonze,[6] with the important difference that our approach generally converges more rapidly and, most importantly, is parameter free.

### F. Range of applicability

In this section we briefly discuss the range of applicability of the EET. As mentioned before, in principle, the EET can be used to rewrite any SOS expression in terms of occupied states only, namely, by the introduction of an effective energy with sufficient degrees of freedom. However, we do not expect that simple approximations to this effective energy will lead to accurate results in all cases.

Let us consider, for example, the imaginary part of the head of the polarizability tensor $\chi^0_{\mathbf{GG}'}(\omega)$. The SOS expression for this element is given by

$$\mathrm{Im}\chi^0_{\mathbf{00}}(\mathbf{q},\omega) = \sum_{v,c} \int d\mathbf{r} \int d\mathbf{r}' \phi_v^*(\mathbf{r})\phi_v(\mathbf{r})\phi_c^*(\mathbf{r}')\phi_v(\mathbf{r}') \times e^{i\mathbf{q}\cdot(\mathbf{r}-\mathbf{r}')}\delta\big(\omega-(\epsilon_c-\epsilon_v)\big), \quad (57)$$

where, for simplicity, we assumed a material with a gap and $\omega > 0$. If we compare this to the EET result using $\delta'^{(0)}$ and $\delta_v'^{(1)}$, we obtain

$$\mathrm{Im}\chi^0_{\mathbf{00}}(\mathbf{q},\omega) = \sum_v f_v^{\rho\rho}(\mathbf{q},\mathbf{0},\mathbf{0})\delta\big(\omega-\delta'^{(0)}(\mathbf{q},\mathbf{0},\mathbf{0})\big), \quad (58)$$

$$\mathrm{Im}\chi^0_{\mathbf{00}}(\mathbf{q},\omega) = \sum_v f_v^{\rho\rho}(\mathbf{q},\mathbf{0},\mathbf{0})\delta\big(\omega-\delta_v'^{(1)}(\mathbf{q},\mathbf{0},\mathbf{0})\big). \quad (59)$$

While Eq. (57) consists of a summation over a number of poles equal to $N_vN_c$, Eq. (58) contains only a single pole while Eq. (59) contains $N_v$ poles. Therefore, with the simple frequency-independent approximations $\delta'^{(0)}$ and $\delta_v'^{(1)}$, we will, in general, not be able to describe $\mathrm{Im}\chi^0_{\mathbf{00}}(\omega)$ in an accurate way. Hence, we expect that the calculation of an accurate absorption spectrum, which is closely related to $\mathrm{Im}\chi^0_{\mathbf{00}}(\omega)$, would require complicated frequency-dependent effective energies far beyond $\delta_v^{(1)}$. We note that, nevertheless, $\chi^0_{\mathbf{00}}(\omega)$ expressed in terms of $\delta_v^{(1)}$ satisfies the high-frequency limit and the generalized $f$-sum rule (see Secs. II D 1 and II D 2).

On the other hand, we expect that quantities which depend on frequency integrals over $\chi^0(\omega)$, such as the $GW$ self-energy, can be accurately reproduced with simple approximations to $\delta_v'(\omega)$, precisely because exact constraints such as the generalized $f$-sum rule and the high-frequency limit are satisfied. Similarly, we expect that summations over $\mathbf{q}$, $\mathbf{G}$, and $\mathbf{G}'$, such as those that occur in the calculation of the self-energy matrix elements, allow us to use relatively simple approximations for $\delta_v(\omega)$.

## III. IMPLEMENTATION

We implemented the EET described above in the ABINIT software package.[29] In this section we would like to discuss two technical details of our implementation.

First, as can be verified from Eqs. (14) and (15), $\Sigma_c^{n,\mathrm{emp}}(\omega)$ does not have poles in the energy range $[-\infty,\epsilon_L+\omega_1]$, where $\epsilon_L$ is the eigenvalue of the lowest empty state and $\omega_1$ is the first neutral excitation energy. In practice, however, the approximations for $\delta_{ng}(\omega)$ given in Eqs. (31)–(33), might lead to spurious poles in this energy range. Therefore, to avoid numerical instabilities, we constrain the effective energy $\epsilon_n+\delta_{ng}(\omega)$ in Eq. (16) to the range $[\epsilon_L,\infty]$; i.e., $\delta_{ng}(\omega)$ is set to $\epsilon_L-\epsilon_n$ in the case that the effective energy $\epsilon_n+\delta_{ng}(\omega)$ obtained using the approximations in Eqs. (39)–(41) results in $\epsilon_n+\delta_{ng}(\omega) < \epsilon_L$. Using the first mean-value theorem for integration,[30] one can show that this constraint is exact for all diagonal elements $\delta_{ng}(\mathbf{q},\mathbf{G},\mathbf{G},\omega)$ since in this case the numerator on the right-hand side of Eq. (15) is non-negative for every $c$.

In standard $GW$ calculations the independent-particle polarizability is evaluated on the imaginary-frequency axis, where it has no poles (excepting metals at $\omega = 0$), and then fitted to a plasmon-pole model (PPM).[23,31] Therefore, similar numerical instabilities as described above might only occur in the evaluation of $\chi^0(i\omega)$ at $\omega = 0$. Since there should be no pole at $\omega = 0$ (for systems with a gap), we constrain $\epsilon_v+\delta_v'(\omega)$ in Eq. (38) to the range $[\epsilon_L,\infty]$ for this frequency in a manner similar to that explained above for $\epsilon_n+\delta_{ng}(\omega)$.

Second, as within the SOS approach, the calculation of the head and wings of the dielectric matrix for $\mathbf{q}\to 0$ requires special attention since for these elements one cannot simply set $\mathbf{q} = 0$. One usually employs $\mathbf{k}\cdot\mathbf{p}$ perturbation theory to evaluate the limit $\mathbf{q}\to 0$ for these elements. However, $\mathbf{k}\cdot\mathbf{p}$ perturbation theory introduces an additional summation over empty states. This can, for example, be avoided by using a small but finite $\mathbf{q}$ or by numerically expanding the wave functions around $\mathbf{q} = 0$.[32] However, since the calculation of the head and wings is an order of magnitude smaller than that of the body and the number of empty states required to reach convergence for these elements is small, we found it more efficient to simply use the SOS approach for the head and wings when $\mathbf{q}\to 0$. The extra computational cost is negligible.

## IV. RESULTS

### A. Computational details

All our calculations were performed using separable norm-conserving pseudopotentials.[33,34] For Sn, the semicore electrons of the $4s$, $4p$, and $4d$ states were considered as

TABLE I. Calculated energies (in eV) for the VBM, CBM, and fundamental gap ($E_g$) of $SnO_2$. The last column contains numerically converged $G^0W^0$ quasiparticle energies. See the text for further details.

| | | $G^0W^0$ | |
|---|---|---|---|
| | LDA | EET | SOS + EET |
| CBM | 8.20 | 8.73 | 8.74 |
| VBM | 7.26 | 5.87 | 5.85 |
| $E_g$ | 0.94 | 2.86 | 2.89 |

valence electrons. Similarly, for Zn, the semicore electrons of the $3s$, $3p$, and $3d$ states were considered as valence electrons.

In the case of $SnO_2$ we used calculcated lattice parameters and atomic positions which we obtained from a density-functional calculation using the local-density approximation (LDA), while in the cases of ZnO and bulk rubrene we used experimental values. To compare with the work of Sai *et al.*,[35] we also performed calculations for the model geometry of bulk rubrene that they introduced. More details are given below.

The $k$-point sampling of the Brillouin zone was carried out with a Monkhorst-Pack (MP) grid.[36] For $SnO_2$ and ZnO we used a $4 \times 4 \times 6$ and $6 \times 6 \times 4$ MP grid, respectively. In the case of bulk rubrene we used a $2 \times 2 \times 2$ and $2 \times 4 \times 2$ MP grid, for the experimental and model geometry, respectively. For the calculation of the self-energy these grids were shifted such that they contain the $\Gamma$ point, while for the calculation of the dielectric matrix they were shifted such that they do not include the $\Gamma$ point. The ground-state cutoff energies for $SnO_2$, ZnO, and bulk rubrene were 240, 350, and 100 Ry, respectively. The cutoff energies for the dielectric matrix for $SnO_2$, ZnO, and bulk rubrene were 48, 80, and 13 Ry, respectively. We used the generalized PPM of Godby and Needs[31] to fit $\epsilon^{-1}(\omega)$.

### B. $SnO_2$

$SnO_2$ has a rutile crystal structure with lattice parameters $a = 4.726$ Å and $c = 3.191$ Å, which we obtained from a DFT-LDA calculation and which agrees well with the experimental values $a = 4.737$ Å and $c = 3.186$ Å.[37] We calculated the $G^0W^0$ quasiparticle energies at the valence band maximum (VBM) and conduction band minimum (CBM) of $SnO_2$, both located at the $\Gamma$ point, with our EET using $\delta'^{(2)}$ and $\delta^{(2)}$ in the calculation of the screening and self-energy, respectively. These values for the VBM and CBM as well as the resulting band gap are reported in Table I.

We would like to compare these values to the quasiparticle energies obtained within the standard SOS approach. However, to obtain numerically converged absolute quasiparticle energies is even more difficult than to obtain numerically converged quasiparticle energy differences such as band gaps. While 1600 empty bands (corresponding to a 32.2-Ry energy cutoff)[38] included in the self-energy calculation were sufficient to reach convergence for the band gap, convergence for the quasiparticle energies at the VBM and CBM was still not reached. Therefore, in order to compare our approximate EET results to numerically converged values, we employed the strategy outlined in Sec. II E to combine the SOS aproach with the EET.

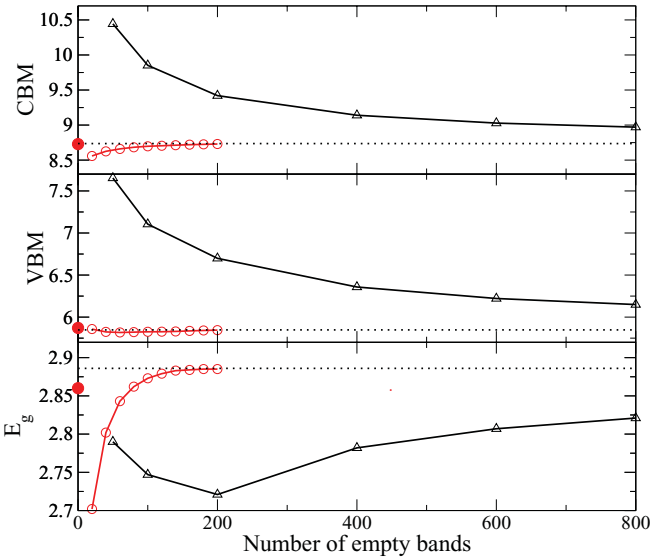


FIG. 1. (Color online) Convergence behavior of the calculated energies (in eV) of the VBM, CBM, and fundamental gap ($E_g$) of $SnO_2$ with the number of empty states in both the screening and the self-energy calculcations. Triangles (black), SOS approach; open (red) circles, SOS + EET approach using $\delta'^{(0)}$ and $\delta^{(0)}$; filled (red) circles, EET using $\delta'^{(2)}$ and $\delta^{(2)}$ without empty states.

As an alternative to the accurate high-order approximations for $\delta'$ and $\delta$, this SOS + EET approach allows us to combine the slightly less accurate but very simple approximations $\delta^{(0)}$ and $\delta'^{(0)}$ given in Eqs. (31) and (39) with the SOS approach using only very few empty states. In Fig. 1 we report the convergence behavior of the calculated energies of the VBM, CBM and band gap of $SnO_2$ with the number of empty states using the standard SOS approach and the SOS+EET approach. We see that using the SOS + EET approach, numerical convergence of 10 meV is reached with slightly more than 100 empty bands (corresponding to a 3.5-Ry energy cutoff).[38] This is true, not only for the band gap, but also for the absolute quasiparticle energies at the VBM and CBM. By contrast, the SOS approach has not reached convergence for any of these quantities with as many as 800 empty bands (corresponding to a 19.6-Ry energy cutoff).[38]

We are now also able to compare the converged SOS + EET results with those obtained with our approximate EET scheme using no empty states. This comparison is reported in Table I. We conclude that the values we obtained with our EET using $\delta'^{(2)}$ and $\delta^{(2)}$ are in excellent agreement with the numerically exact values.[39]

### C. ZnO

Recently there has been much debate about the numerically exact value of the $G^0W^0$ band gap of ZnO. This discussion started with the publication of the work by Shih *et al.*[40] in which the authors claimed that the $G^0W^0$ band gap of ZnO is at least 3.4 eV. This value is significantly larger than previously reported values, which were in the range of 2.1–2.6 eV.[41–44] The explanation by Shih *et al.* is an extremely slow convergence of the band gap with the number of empty states included in the calculation of the self-energy. To obtain a band

TABLE II. Calculated energies (in eV) for the VBM, CBM, and fundamental gap ($E_g$) of ZnO. The last column contains numerically converged $G^0W^0$ quasiparticle energies. See the text for further details.

| | | $G^0W^0$ | |
|---|---|---|---|
| | LDA | EET | SOS + EET |
| VBM | 6.38 | 5.04 | 4.97 |
| CBM | 7.19 | 7.43 | 7.53 |
| $E_g$ | 0.82 | 2.39 | 2.56 |

gap of 3.4 eV they had to include 3000 empty bands in their self-energy calculation. Subsequent calculations using the full-potential linear augmented-plane-wave (FLAPW) method[45] performed by Friedrich *et al.*[46] confirmed the extremely slow convergence of the ZnO band gap with the number of empty states. However, the band gap of 2.83 eV that they obtained by extrapolating to an infinite number of empty states was substantially lower than the 3.4 eV found by Shih *et al.* Recently it was shown by Stankovski *et al.*[47] that the main reason for the large discrepancy between the band gap obtained by Shih *et al.* and those obtained in the other works is due to the PPM of Hybertsen and Louie,[23] which was adopted by Shih *et al.* but not by the others. Stankovski *et al.* showed that the use of the Hybertsen-Louie PPM leads to a large overestimation of the $G^0W^0$ band gap of ZnO. They also showed that the ZnO band gap obtained using the Godby-Needs PPM[31] agrees very well with the band gap obtained from a calculation which avoids the use of a PPM. Nevertheless, also the band gaps obtained without a PPM and with the Godby-Needs PPM show a very slow convergence with the number of empty states. These works motivated us to study ZnO with the EET, in which the summation over empty states can be avoided.

ZnO has a wurtzite crystal structure with lattice parameters $a = 3.249$ Å and $c = 5.207$ Å.[48] In Table II we report the $G^0W^0$ band gap of ZnO as well as the absolute $G^0W^0$ quasiparticle energies at the VBM and CBM, which are both located at the Γ point obtained with the EET using $\delta'^{(2)}$ and $\delta^{(2)}$ in the calculation of $W$ and Σ, respectively. To compare these values to numerically converged $G^0W^0$ energies, once again, we use the SOS + EET approach since also for ZnO the SOS approach alone converges extremely slowly with respect to the number of empty bands. In Fig. 2 we report the convergence behavior of the calculated energies of the VBM, CBM, and band gap of ZnO with the number of empty states using the standard SOS approach and the SOS + EET approach. We see that the band gap using the SOS + EET approach does not converge as quickly as was the case for $SnO_2$ but convergence is still reached much faster than with the SOS approach alone. We conclude that the converged $G^0W^0$ band gap of ZnO is 2.56 eV. The difference with respect to the extrapolated FLAPW result of Friedrich *et al.* is less than 0.3 eV.

We can now compare the converged SOS + EET results with those obtained with our approximate EET scheme using no empty states. We report this comparison in Table II. We conclude that the absolute quasiparticle energies at the VBM and CBM that we obtained with our EET using $\delta'^{(2)}$ and $\delta^{(2)}$ are in very good agreement with the numerically exact values.

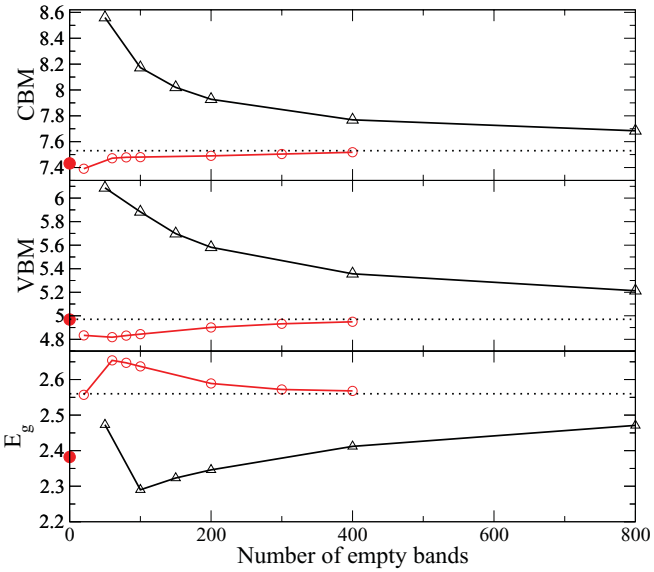


FIG. 2. (Color online) Convergence behavior of the calculated energies (in eV) of the VBM, CBM, and fundamental gap ($E_g$) of ZnO with the number of empty states in both the screening and the self-energy calculations. Triangles (black), SOS approach; open (red) circles, SOS + EET approach using $\delta'^{(0)}$ and $\delta^{(0)}$; filled (red) circles, EET using $\delta'^{(2)}$ and $\delta^{(2)}$ without empty states.

Due to the fact that the VBM energy is slightly underestimated while the CBM energy is slightly overestimated, the difference between the resulting EET band gap and the numerically exact $G^0W^0$ gap is slightly larger for ZnO than for $SnO_2$ and the other materials we have studied in a previous work.[21] However, with ∼5% deviation, we can still consider the agreement good.

### D. Bulk rubrene

Now that we have verified the accuracy of the EET we can safely apply it to predict the band gaps of larger systems, which are cumbersome to treat with the standard SOS approach. Here we study bulk rubrene, an organic molecular crystal. Rubrene is an interesting material with many technological applications, for example, in organic light-emitting diodes and organic field-effect transistors to create flexible electronics,[49] but is computationally challenging due to the large number of atoms involved.

Crystalline rubrene has an orthorhombic unit cell with lattice parameters $a = 14.4$ Å, $b = 7.2$ Å, and $c = 26.8$ Å.[50] Each unit cell contains two identical $ab$ planes separated by $c/2$, with a relative shift between the planes of $b/2$. Therefore, the unit cell of bulk rubrene contains two rubrene molecules, for a total of 140 atoms per unit cell. To the best of our knowledge, the only $GW$ calculation on bulk rubrene was carried out by Sai *et al.*[35] However, to reduce the cost of their calculations, the authors used a model geometry for the rubrene unit cell in which they neglected the relative shift of the two $ab$ planes. This allowed them to use a reduced unit cell with lattice parameters $a = 14.4$ Å, $b = 7.2$ Å, and $c = 14.4$ Å. They expected that the interactions between rubrene molecules in adjacent $ab$ planes is weak and therefore relatively insensitive to the relative shift of the two planes. They then further justified this approximation by showing that the band gap

TABLE III. Fundamental gap ($E_g$; in eV) of bulk rubrene within $G^0W^0$. Details of the model are explained in the text.

| | EET | EET (model) | Ref. 35 (model) |
|---|---|---|---|
| $E_g$ | 2.5 | 2.9 | 2.8 |

they obtain for the model geometry (1.20 eV) is only slightly larger than the band gap of the experimental geometry (1.14 eV) when calculated within DFT using a generalized-gradient approximation (GGA).

In this work the DFT ground-state calculcations are performed within the LDA. However, the DFT-LDA band gaps that we obtain, i.e., 1.13 and 1.20 eV for the experimental and model geometry, respectively, are in very close agreement with the DFT-GGA band gaps reported by Sai *et al*., i.e., 1.14 and 1.20 eV. We therefore assume that a comparison between our $G^0W^0$ results and those of Sai *et al*. will not be hindered by this difference in the ground-state calculation.

In Table III we report the $G^0W^0$ band gaps of bulk rubrene that we obtained with the EET, using $\delta'^{(2)}$ and $\delta^{(2)}$, for the experimental and model geometry as well as the $G^0W^0$ band gap obtained by Sai *et al*. for the model geometry. We see that the band gap we obtain for the model geometry is in good agreement with that found by Sai *et al*. With the EET we can now also calculate the band gap for the unit cell with the experimental geometry containing 140 atoms. This results in a band gap of 2.5 eV, which is 0.4 eV smaller than that for the model geometry. This indicates that the interactions between adjacent $ab$ planes are not weak and therefore the relative shift of these planes cannot be neglected.

## V. CONCLUSIONS

The scope of this work is multifold. First, we have given further details of the EET, a simple method we introduced recently[21] to evaluate spectral representations in an accurate and efficient manner without summing over empty states as is done in the standard SOS approach. In particular, we showed how the EET can be applied to reformulate the expressions for the $GW$ self-energy and the independent-particle polarizability in terms of occupied states only by introducing a single effective energy which takes into account all the empty states. Second, we provided further evidence of the accuracy of the EET by showing that quasiparticle energies and band gaps obtained with $GW$ using the EET agree well with those obtained using the standard SOS approach. Third, with the EET we were able to resolve the problem of the slow convergence of the ZnO band gap with the number of empty states in a $GW$ calculation. Fourth, thanks to the EET, we could predict the band gap of bulk rubrene, a technologically interesting material for inorganic devices with a 140-atom unit cell.

Finally, the results obtained in this and a previous work[21] have shown that, with the EET, we obtain accurate results for a large variety of systems: an $sp$ semiconductor (Si), a wide-gap insulator (solid Ar), an atom (Ar), $d$-band semiconductors ($SnO_2$, ZnO), and an organic molecular crystal (rubrene).


## ACKNOWLEDGMENTS

We thank János Ángyán, Friedhelm Bechstedt, Christoph Friedrich, Matteo Giantomassi, Xavier Gonze, John Rehr, Andreas Savin, and Martin Stankovski for helpful discussions. We thank Julien Vidal for providing us with the pseudopotential of Zn. We acknowledge funding from Triangle de la Physique under Contract No. 2007-71, Saint-Gobain R&D under Contract No. 091986, the European Community's FP7 under Grant No. 211956, and the ANR under Project No. NT09-610745.


## APPENDIX A: NONLOCAL POTENTIALS

In the case where the Hamiltonian in Eq. (19) contains an additional nonlocal potential $v_{nl}(\mathbf{r},\mathbf{r}')$, the expression for $\tilde{j}_{cn}$ in Eq. (23) is slightly modified:

$$\begin{aligned}\tilde{j}_{cn}(\mathbf{q}+\mathbf{G}) = {} & \langle c|e^{-i(\mathbf{q}+\mathbf{G})\cdot\mathbf{r}}[i\nabla_{\mathbf{r}}]|n\rangle\cdot(\mathbf{q}+\mathbf{G}) \\ & + \int d\mathbf{r}d\mathbf{r}'\phi_c^*(\mathbf{r})v_{nl}(\mathbf{r},\mathbf{r}') \\ & \times [e^{-i(\mathbf{q}+\mathbf{G})\cdot\mathbf{r}'} - e^{-i(\mathbf{q}+\mathbf{G})\cdot\mathbf{r}}]\phi_n(\mathbf{r}'). \quad \text{(A1)}\end{aligned}$$

If $v_{nl}$ refers to the nonlocal part of a separable pseudopotential, i.e., $v_{nl}(\mathbf{r},\mathbf{r}') = \sum_s \tilde{v}_s(\mathbf{r})\tilde{v}_s(\mathbf{r}')$, the last term on the right-hand side of Eq. (A1) can be written as

$$\begin{aligned}&\int d\mathbf{r}d\mathbf{r}'\phi_c^*(\mathbf{r})v_{nl}(\mathbf{r},\mathbf{r}')[e^{-i(\mathbf{q}+\mathbf{G})\cdot\mathbf{r}'} - e^{-i(\mathbf{q}+\mathbf{G})\cdot\mathbf{r}}]\phi_n(\mathbf{r}') \\ &= \sum_s \int d\mathbf{r}\phi_c^*(\mathbf{r})\tilde{v}_s(\mathbf{r}) \int d\mathbf{r}'\tilde{v}_s(\mathbf{r}')e^{-i(\mathbf{q}+\mathbf{G})\cdot\mathbf{r}'}\phi_n(\mathbf{r}') \\ &\quad - \sum_s \int d\mathbf{r}\phi_c^*(\mathbf{r})e^{-i(\mathbf{q}+\mathbf{G})\cdot\mathbf{r}}\tilde{v}_s(\mathbf{r}) \int d\mathbf{r}'\tilde{v}_s(\mathbf{r}')\phi_n(\mathbf{r}'), \quad \text{(A2)}\end{aligned}$$

which can be rapidly calculated in practice. In the case of pseudopotentials of the Kleinman-Bylander type,[33] the index $s$ in the above expression is the multi-index $s = nlm$, where $n$ is the number of the atom, $l$ is the orbital angular momentum quantum number, and $m$ is the magnetic quantum number.

## APPENDIX B: A HOMOGENEOUS ELECTRON GAS

Here we show that $\delta_{ng}(\omega)$ and $\tilde{\delta}_{ng}(\omega)$ as defined in Eqs. (16) and (24), respectively, are equal in the case of a homogeneous electron gas. Combining Eqs. (15) and (16) and making use of the fact that the wave functions can be expressed in terms of a single plane wave, i.e., $\phi_{i\mathbf{k}}(\mathbf{r}) = e^{i(\mathbf{k}+\mathbf{G}_i)\cdot\mathbf{r}}$ (we made the $\mathbf{k}$ dependence explicit), we obtain

$$\begin{aligned}&\delta_{ng}^{\text{hom}}(\mathbf{G},\omega) \\ &= \omega_{ng} - \sum_c \delta(\mathbf{G}_n - \mathbf{G} - \mathbf{G}_c)\left[\sum_{c'} \frac{\delta(\mathbf{G}_n - \mathbf{G} - \mathbf{G}_{c'})}{\omega_{c'g}}\right]^{-1}. \quad \text{(B1)}\end{aligned}$$

In a similar manner, by combining Eqs. (22) and (24) we get

$$\tilde{\delta}^{\rm hom}_{ng}(\mathbf{G},\omega) = \omega_{ng} - \sum_c \delta(\mathbf{G}_n - \mathbf{G} - \mathbf{G}_c)\left[\sum_{c'} \frac{\delta(\mathbf{G}_n - \mathbf{G} - \mathbf{G}_{c'})}{\omega_{c'g}}\right]^{-1}. \quad \text{(B2)}$$

Therefore $\delta^{\rm hom}_{ng}(\mathbf{G},\omega) = \tilde{\delta}^{\rm hom}_{ng}(\mathbf{G},\omega)$. Similarly, one can show that $\delta^{\rm hom}_{ng}(\mathbf{G},\omega) = \tilde{\tilde{\delta}}^{\rm hom}_{ng}(\mathbf{G},\omega)$, etc. This also proves that the approximations given in Eqs. (32) and (33) are exact in the limit of a homogeneous electron gas. The same properties can be shown to hold for $\delta'_v(\omega)$ and $\tilde{\delta}'_v(\omega)$, etc.

## APPENDIX C: A SIMPLIFIED EET FOR $\chi^0(\omega)$

One can obtain an even simpler expression for $\chi^0(\omega)$ if, instead of approximating $X_v(\omega)$, as is done in the EET, we approximate $\sum_v n_v X_v(\omega)$. We can rewrite this term according to

$$\sum_v n_v X_v(\mathbf{q},\mathbf{G},\mathbf{G}',\omega) = \frac{\sum_v n_v f_v^{\rho\rho}(\mathbf{q},\mathbf{G},\mathbf{G}')}{\omega - \Delta'(\mathbf{q},\mathbf{G},\mathbf{G}',\omega) + i\eta}, \quad \text{(C1)}$$

which defines $\Delta'(\mathbf{q},\mathbf{G},\mathbf{G}',\omega)$. We note that such a function can always be found since $\Delta(\mathbf{q},\mathbf{G},\mathbf{G}',\omega)$ has the same degrees of freedom as the left-hand side of Eq. (C1). The quantity $\Delta'(\omega)$ fulfills the same purpose as $\delta'_v(\omega)$ in Eq. (38) but is simpler since it is independent of $v$. Following a derivation similar to the one that led to Eqs. (39)–(41), we obtain the following approximations for $\Delta'(\omega)$:

$$\Delta'^{(0)}(\mathbf{q},\mathbf{G},\mathbf{G}') = Q(\mathbf{q},\mathbf{G},\mathbf{G}'), \quad \text{(C2)}$$

$$\Delta'^{(1)}(\mathbf{q},\mathbf{G},\mathbf{G}') = Q(\mathbf{q},\mathbf{G},\mathbf{G}') + \frac{F^{\rho j}(\mathbf{q},\mathbf{G},\mathbf{G}')}{F^{\rho\rho}(\mathbf{q},\mathbf{G},\mathbf{G}')}, \quad \text{(C3)}$$

$$\Delta'^{(2)}(\mathbf{q},\mathbf{G},\mathbf{G}',\omega) = Q(\mathbf{q},\mathbf{G},\mathbf{G}') + \frac{F^{\rho j}(\mathbf{q},\mathbf{G},\mathbf{G}')}{F^{\rho\rho}(\mathbf{q},\mathbf{G},\mathbf{G}')} \times \left[\frac{\omega - Q(\mathbf{q},\mathbf{G},\mathbf{G}') - \frac{F^{\rho j}(\mathbf{q},\mathbf{G},\mathbf{G}')}{F^{\rho\rho}(\mathbf{q},\mathbf{G},\mathbf{G}')}}{\omega - Q(\mathbf{q},\mathbf{G},\mathbf{G}') - \frac{F^{jj}(\mathbf{q},\mathbf{G},\mathbf{G}')}{F^{\rho j}(\mathbf{q},\mathbf{G},\mathbf{G}')}}\right], \quad \text{(C4)}$$

where $F^{\rho\rho} = \sum_v n_v f_v^{\rho\rho}$, etc. The quantities $F^{\rho\rho}$, $F^{\rho j}$, and $F^{jj}$, which appear in the above equations as well as in the numerator of Eq. (C1), just depend on (Fourier transforms of) the density and the KS or (noninteracting) quasiparticle one-body reduced density matrix:

$$F^{\rho\rho}(\mathbf{q},\mathbf{G},\mathbf{G}') = \rho(\mathbf{G}' - \mathbf{G}) - \int d\mathbf{r}d\mathbf{r}' e^{i(\mathbf{q}+\mathbf{G})\cdot\mathbf{r}} e^{-i(\mathbf{q}+\mathbf{G}')\cdot\mathbf{r}'} |\rho(\mathbf{r},\mathbf{r}')|^2, \quad \text{(C5)}$$

$$F^{\rho j}(\mathbf{q},\mathbf{G},\mathbf{G}') = \frac{i}{2} P(\mathbf{q},\mathbf{G},\mathbf{G}')\cdot(\mathbf{q}+\mathbf{G}') + \text{H.c.}, \quad \text{(C6)}$$

$$F^{jj}(\mathbf{q},\mathbf{G},\mathbf{G}') = (\mathbf{q}+\mathbf{G})\cdot\tilde{P}(\mathbf{q},\mathbf{G},\mathbf{G}')\cdot(\mathbf{q}+\mathbf{G}'), \quad \text{(C7)}$$

where

$$P(\mathbf{q},\mathbf{G},\mathbf{G}') = \int d\mathbf{r} e^{i(\mathbf{G}-\mathbf{G}')\cdot\mathbf{r}} \nabla_{\mathbf{r}} \rho(\mathbf{r}) - \int d\mathbf{r}d\mathbf{r}' e^{i(\mathbf{q}+\mathbf{G})\cdot\mathbf{r}} e^{-i(\mathbf{q}+\mathbf{G}')\cdot\mathbf{r}'} \nabla_{\mathbf{r}'} |\rho(\mathbf{r},\mathbf{r}')|^2, \quad \text{(C8)}$$

$$\tilde{P}(\mathbf{q},\mathbf{G},\mathbf{G}') = \int d\mathbf{r} e^{i(\mathbf{G}-\mathbf{G}')\cdot\mathbf{r}} \nabla_{\mathbf{r}}\nabla_{\mathbf{r}} \rho(\mathbf{r}) - \int d\mathbf{r}d\mathbf{r}' e^{i(\mathbf{q}+\mathbf{G})\cdot\mathbf{r}} e^{-i(\mathbf{q}+\mathbf{G}')\cdot\mathbf{r}'} \rho(\mathbf{r},\mathbf{r}') \nabla_{\mathbf{r}}\nabla_{\mathbf{r}'} \rho(\mathbf{r},\mathbf{r}'). \quad \text{(C9)}$$

The above approximations for $\Delta'(\omega)$ as well as the corresponding approximations for $\chi^0(\omega)$ (for systems with a gap) are explicit functionals of a one-body reduced density matrix. Therefore, they could also be useful in the modeling of density-matrix functionals or polarizabilities. The latter could then be used to calculate efficiently total energies.[51]

We note that the $\chi^0(\omega)$ that result from using the EET with $\delta'^{(0)}$ and $\Delta'^{(0)}$ are identical. While the overall scaling of the EET approach presented in the previous sections is, in general, $N_{\rm at}^3 \log N_{\rm at}$,[21] the scaling of this simplified EET scheme is $N_{\rm at}^3$, where $N_{\rm at}$ is the number of atoms. This scaling is an order of magnitude smaller than the $N_{at}^4$ scaling of the standard SOS approach.

*arjan.berger@irsamc.ups-tlse.fr


[1] L. Hedin, Phys. Rev. A **139**, 796 (1965).
[2] W. G. Aulbur, L. Jönsson, and J. W. Wilkins, in *Solid State Physics* (Academic, New York, 2000), Vol. 54, p. 1.
[3] L. Steinbeck, A. Rubio, L. Reining, M. Torrent, I. White, and R. Godby, Comput. Phys. Commun. **125**, 105 (2000).
[4] M. L. Tiago, S. Ismail-Beigi, and S. G. Louie, Phys. Rev. B **69**, 125212 (2004).
[5] M. van Schilfgaarde, T. Kotani, and S. V. Faleev, Phys. Rev. B **74**, 245125 (2006).
[6] F. Bruneval and X. Gonze, Phys. Rev. B **78**, 085125 (2008).
[7] M. E. Casida and D. P. Chong, Phys. Rev. A **40**, 4837 (1989); **44**, 6151 (1991).
[8] F. Bechstedt, R. Del Sole, G. Cappellini, and L. Reining, Solid State Commun. **84**, 765 (1992).
[9] S. Baroni and A. Quattropani, Nuovo Cimento D **5**, 89 (1985).
[10] S. Baroni, P. Giannozzi, and A. Testa, Phys. Rev. Lett. **58**, 1861 (1987).
[11] L. Reining, G. Onida, and R. W. Godby, Phys. Rev. B **56**, R4301 (1997).
[12] H. F. Wilson, F. Gygi, and G. Galli, Phys. Rev. B **78**, 113303 (2008).
[13] H. F. Wilson, D. Lu, F. Gygi, and G. Galli, Phys. Rev. B **79**, 245106 (2009).
[14] P. Umari, G. Stenuit, and S. Baroni, Phys. Rev. B **81**, 115104 (2010).
[15] F. Giustino, M. L. Cohen, and S. G. Louie, Phys. Rev. B **81**, 115105 (2010).

[16]W. Kang and M. S. Hybertsen, Phys. Rev. B **82**, 195108 (2010).
[17]P. Umari, G. Stenuit, and S. Baroni, Phys. Rev. B **79**, 201104(R) (2009).
[18]X. Blase, C. Attaccalite, and V. Olevano, Phys. Rev. B **83**, 115103 (2011).
[19]D. Foerster, P. Koval, and D. Sánchez-Portal, J. Chem. Phys. **135**, 074105 (2011).
[20]G. Samsonidze, M. Jain, J. Deslippe, M. L. Cohen, and S. G. Louie, Phys. Rev. Lett. **107**, 186404 (2011).
[21]J. A. Berger, L. Reining, and F. Sottile, Phys. Rev. B **82**, 041103(R) (2010).
[22]L. Hedin, J. Phys. Condensed Matter **11**, R489 (1999).
[23]M. S. Hybertsen and S. G. Louie, Phys. Rev. B **34**, 5390 (1986).
[24]R. W. Godby, M. Schlüter, and L. J. Sham, Phys. Rev. B **37**, 10159 (1988).
[25]P. Hohenberg and W. Kohn, Phys. Rev. **136**, B864 (1964).
[26]W. Kohn and L. J. Sham, Phys. Rev. **140**, A1133 (1965).
[27]O. V. Gritsenko and E. J. Baerends, Phys. Rev. A **64**, 042506 (2001).
[28]D. L. Johnson, Phys. Rev. B **9**, 4475 (1974).
[29]X. Gonze, G. Rignanese, M. Verstraete, J. Beuken, Y. Pouillon, R. Caracas, F. Jollet, M. Torrent, G. Zerah, M. Mikami *et al.*, Z. Kristallogr. **220**, 558 (2005).
[30]H. von Mangoldt and K. Knopp, *Einführung in die höhere Mathematik* (S. Hirzel Verlag, Stuttgart, 1948).
[31]R. W. Godby and R. J. Needs, Phys. Rev. Lett. **62**, 1169 (1989).
[32]X. Gonze, Phys. Rev. B **55**, 10337 (1997).
[33]L. Kleinman and D. M. Bylander, Phys. Rev. Lett. **48**, 1425 (1982).
[34]N. Troullier and J. L. Martins, Phys. Rev. B **43**, 1993 (1991).
[35]N. Sai, M. L. Tiago, J. R. Chelikowsky, and F. A. Reboredo, Phys. Rev. B **77**, 161306 (2008).
[36]H. J. Monkhorst and J. D. Pack, Phys. Rev. B **13**, 5188 (1976).
[37]R. W. G. Wyckoff, *Crystal Structures 1* (Interscience, New York, 1963).
[38]The reported energy cut-off is relative to the CBM.
[39]The small differences in the band gaps of $SnO_2$ reported in this work and those reported in a previous work (Ref. 21) are due to a denser **k**-space sampling of the Brillouin zone in the present work.
[40]B.-C. Shih, Y. Xue, P. Zhang, M. L. Cohen, and S. G. Louie, Phys. Rev. Lett. **105**, 146401 (2010).
[41]M. Usuda, N. Hamada, T. Kotani, and M. van Schilfgaarde, Phys. Rev. B **66**, 125101 (2002).
[42]M. Shishkin and G. Kresse, Phys. Rev. B **75**, 235102 (2007).
[43]F. Fuchs, J. Furthmüller, F. Bechstedt, M. Shishkin, and G. Kresse, Phys. Rev. B **76**, 115109 (2007).
[44]P. Gori, M. Rakel, C. Cobet, W. Richter, N. Esser, A. Hoffmann, R. Del Sole, A. Cricenti, and O. Pulci, Phys. Rev. B **81**, 125207 (2010).
[45]E. Wimmer, H. Krakauer, M. Weinert, and A. J. Freeman, Phys. Rev. B **24**, 864 (1981).
[46]C. Friedrich, M. C. Müller, and S. Blügel, Phys. Rev. B **83**, 081101(R) (2011); **84**, 039906(E) (2011).
[47]M. Stankovski, G. Antonius, D. Waroquiers, A. Miglio, H. Dixit, K. Sankaran, M. Giantomassi, X. Gonze, M. Côté, and G.-M. Rignanese, Phys. Rev. B **84**, 241201(R) (2011).
[48]Y.-N. Xu and W. Y. Ching, Phys. Rev. B **48**, 4335 (1993).
[49]T. Hasegawa and J. Takeya, Sci. Technol. Adv. Mater. **10**, 024314 (2009).
[50]O. D. Jurchescu, A. Meetsma, and T. T. M. Palstra, Acta Crystallogr. B **62**, 330 (2006).
[51]D. C. Langreth and J. P. Perdew, Solid State Commun. **17**, 1425 (1975).